Trans Indian Inst Met (2020) 73(6):1595–1603
https://doi.org/10.1007/s12666-020-01941-9

ORIGINAL ARTICLE

Thermodynamic Assessment of Steelmaking Practices for the Production of Re-sulfur Steels

T. S. Prithiv[1,3] · G. Thirumurugan[1,4] · M. Madan[2] · Ashok Kamaraj[2]

Received: 18 December 2019 / Accepted: 5 March 2020 / Published online: 21 March 2020

Abstract FactSage has become one of the most important modeling tools in simulating the high-temperature metallurgical processes. The usefulness of the FactSage has been demonstrated in this work using several examples of steelmaking processes. Primary steelmaking (basic oxygen furnace) simulation was done with the available process data, and process charts similar to the standard ones were obtained. Ladle refining furnace process for free-cutting steels was simulated and it was observed that absolute non-equilibrium condition exists in steel during casting due to S injection. It was found that non-metallic inclusion formation is thermodynamically possible at final processing stages during Ca and S injection with variable recoveries. A significant change in the nature of non-metallic inclusions formed in re-sulfur steel causes clogging during continuous casting of liquid steel, and its influence on the process has been discussed, for mere 2 ppm of Ca difference in the liquid steel composition.

Keywords Free-cutting steels · Clogging · Non-metallic inclusions · Castability

✉ Ashok Kamaraj
srhsbioboy@yahoo.co.in; ashokk@nmlindia.org

[1] Department of Metallurgical Engineering, Government College of Engineering, Salem, India

[2] Metal Extraction and Recycling Division, CSIR-National Metallurgical Laboratory, Jamshedpur, Jharkhand, India

[3] Present Address: Max-Planck-Institut für Eisenforschung, Max-Planck-Str. 1, 40237 Düsseldorf, Germany

[4] Present Address: Bharat Forge Ltd, Pune, India

1 Introduction

Thermodynamics of materials, as well as processes, are well understood, and tools for thermodynamic analysis have been developed over the last 6–7 decades. The application of thermodynamic concepts for futuristic prediction of high-temperature phenomena becomes a fascinating study in metallurgical industries. It plays a major role in knowing the limits of chemical reactions such as slag–metal, inclusion–metal, refractory–metal and gas–metal reactions in metallurgical reactors. As these processes usually involve high temperature, they impose sampling constraints during industrial experiments [1]. Therefore, the design of metallurgical processes, as well as novel alloys, requires a critical thermodynamic analysis prior to actual experimentation. Commercially available thermodynamic software packages for process analysis purpose are Thermocalc, FactSage, MTDATA, etc. Among the available software packages, FactSage is extensively used for the simulation of high-temperature metallurgical phenomena such as ironmaking, steelmaking [2, 3] and non-ferrous extraction of metals such as Mg, Cu and Al [4, 5].

FactSage databases are very powerful to explore the various refining reactions that occur during liquid steel treatment in primary and secondary steelmaking sections [5]. Secondary steelmaking, as well as ladle metallurgy, involves deoxidation, desulfurization, alloying, vacuum degassing and core wire injection for clean steel practice. Low-alloy steels produced through ladle vacuum degassing route (VD) needs a critical attention during production practice [6–8]. Effective equilibrium reaction zone (EERZ) model [3] has been proposed for simulation of ladle furnace using FactSage Macro processing to mimic the composition evolution during liquid steel treatment.

Several studies [9, 10] have been conducted to simulate the evolution of non-metallic inclusions with and without calcium treatment [9, 11–13].

The present investigation deals with the systematic simulation of basic oxygen furnace and ladle metallurgy process of low-alloy steel using FactSage software. The results have been validated with the literature and industry data to improve the understanding of the refining processes. Two special steel grades have been taken for the current investigation and they are low-carbon (LCRSS) and medium-carbon re-sulfur steels (MCRSS) for fastneres application in the automotives. The production of such grades often show clogging of submerged entry nozzle (SEN) during continuous casting process. It has been found that non-metallic inclusions lead to such problems and therefore, in this study, special attention is given to calcium and sulfur wire injection.

2 Plant Practice and Data Collection

Re-sulfur/machinability grade steels come under the domain of low-alloy steels. Blast furnace (BF) – basic oxygen furnace (BOF) – ladle refining furnace (LRF) – vacuum degassing (VD) – LRF – continuous casting machine (CCM) route is followed by an integrated steel plant to produce re-sulfur steels. Generally, hot metal from BF contains 4 wt.% C; therefore, a major concern of BOF is to remove C and P by blowing oxygen, and thus, the crude steel produced ends up with high amount of dissolved oxygen. Tapped liquid steel from BOF is taken to LRF for further alloying and refining in the ladle. After achieving 90% of aimed chemistry in the LRF, liquid steel is treated in tank vacuum degasser to remove dissolved gases such as nitrogen and hydrogen. Final trimming additions and superheat requirements for casting low-alloy steel are handled at LRF. During all such secondary operations, extensive care is taken to make the liquid steel as clean as possible. Both Ca and S wire injections are carried out at LRF with utmost care and the ladle is lifted to CCM for casting. Argon shrouding for ladle nozzle was provided to avoid re-oxidation of liquid steel. The industrial heat was thoroughly followed from tapping to wire injection and liquid steel samples were collected. The standard sampling procedure was adopted, and the obtained lollypop samples were air-cooled followed by water quenching.

Collected eight samples (4 sample per each heat (LCRSS and MCRSS)) were cut to the desired size (10 mm × 10 mm). These samples were used for further characterization using optical microscope and SEM coupled with EDS (Hitachi S-3400 N) after careful sample preparation. Thermo Electron NSS-300 model of EDS was used for determination of elemental composition of various inclusions with an acceleration voltage of 15 kV.

3 Simulation Procedure

The principle of FactSage calculation is based on Gibbs' free energy minimization technique, which actually predicts the phases for the given thermodynamic conditions. Phase prediction, as well as the feasibility of reaction, can be coupled in FactSage using equilibrium module for simulating high-temperature metallurgical phenomenon. Databases such as FactPS, FToxid and FSstel for pure substances, oxides and liquid steel are used for FactSage simulation, respectively. Equilibrium module of FactSage was employed with these databases to simulate the steelmaking processes in the present investigation. Industry data obtained from BOF and ladle furnace operations were used as an input for the FactSage simulation.

Table 1 shows the initial composition of hot metal along with other important parameters considered in the calculation. Table 2 shows the amount of iron ore addition along with percentage blow at which addition was done. The temperature of the melt during the refining operation was considered to linearly increase with the blow time. Percentage blow was converted into minutes, and isothermal equilibrium calculations were performed for every single minute. Further, the calculated temperature at that time was used for analysis. Therefore, BOF operation was simulated for total processing time and iron ore additions were made at the respective blow period.

During tapping of crude liquid steel from BOF, alloying elements and deoxidizers such as silicon manganese, ferro-silicon, high-carbon ferro-chrome and lime were added in the transfer ladle. The initial composition of crude steel was assumed, and simulation was carried out considering the addition inputs obtained from the industrial tapping process. The initial composition for starting up the FactSage simulations obtained from industry is given in Table 3. LRF process simulation was carried out similarly considering the addition details of ferro-alloys obtained from industry at the different time intervals. Calcium has high affinity toward sulfur than oxygen; it tends to form CaS inclusion, which has the melting point of 2525°C. It may be noted that the Ca and S injection simulation using FactSage in equilibrium module will not be the true representative, unless the slag part is removed for calculation. Therefore, slag–metal equilibrium was neglected during the simulation of Ca and S injection in FactSage simulations. After every equilibrium calculation, the composition of steel and slag was noted for further analysis.

Table 1 Input parameters for BOF simulation

Heat no	Si wt (%)	P	S	Temp (°C)	HM weight Metric tons	Scrap	Lime	Iron Ore	Dolomite	O_2 Nm^3
1	0.82	0.15	0.003	1361	160.6	11.2	12.29	9.15	0	7338
2	0.81	0.152	0.008	1358	151.2	12.7	11.26	12	1.58	7045

Table 2 Iron ore addition in BOF process

Heat no.	% Blow	1st ore addition kg	% Blow	2nd ore addition kg	% Blow	3rd ore addition kg	% Blow	4th Ore addition kg	End blow temp °C
1	37	5002	72	1131	88	561	89	2461	1674
2	46	4663	47	1857	87	5483	Nil	Nil	1629

Table 3 Composition of liquid steel considered as starting composition for LRF simulation obtained from industry

Grade	C (wt.%)	Si	Mn	P	S	Cr	O
LCRSS	0.034	–	–	0.013	0.026	–	0.11
MCRSS	0.065	–	–	0.014	0.035	–	0.127

4 Results and Discussion

Figure 1a shows the simulated results of BOF process, variation in hot metal composition for increasing percent blow for heat 1. The composition profile almost follows the conventional trend reported elsewhere [1]. Silicon gets removed in the early stage of blow and reaches zero within 2 to 3 min, showing its inherent ability to get oxidized. Carbon gradually decreases during the initial stages of blow and in later stages oxidize rapidly. Phosphorous removal is delayed by 10 to 12 min, as it depends on slag nature [14]. Phosphorous then starts to oxidize, as high basic FeO-saturated slag starts to form in the later stages of BOF refining [5]. It is evident from the profile that phosphorous removal needs significant amount of FeO in the slag, which actually decreases the yield of BOF process. Manganese removal does not take place for entire blow pattern, whereas it decreases at the final stage due to

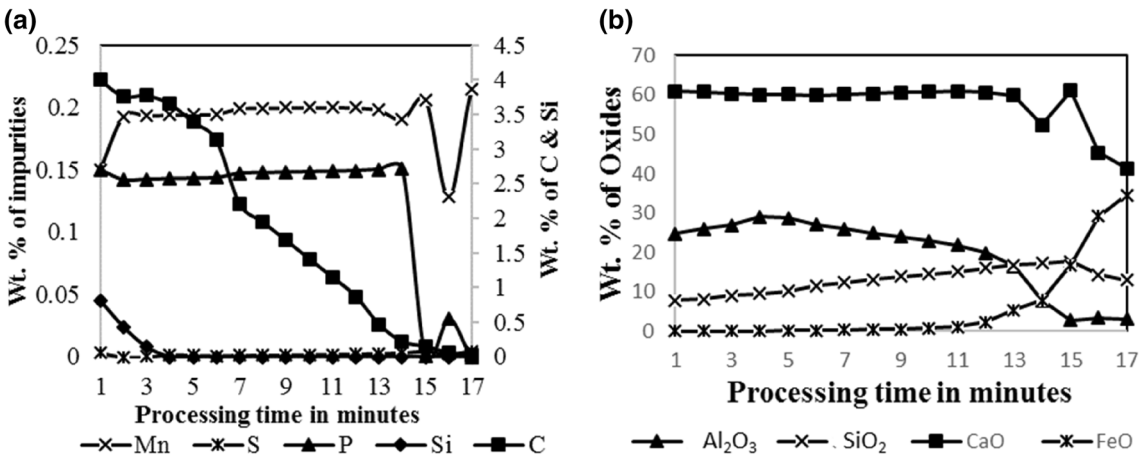

Fig. 1 FactSage-predicted hot metal **a** and slag **b** composition profile of BOF for heat 1

very high oxidizing potential of slag. As expected, sulfur reduction has not taken place and dissolved oxygen in the bath increases rapidly during end blow and attains the saturation.

Figure 1b shows the FactSage-predicted composition of slag throughout the blow time for heat 1. This is also of prime importance to understand the BOF efficiency and to run the process smoothly. The weight percent of lime is always high, as it is added in the initial stage of the process to maintain the basicity high enough for impurities removal. The weight percent of FeO is being constant for almost 10 min and then it increases drastically, as the bath gets depleted in carbon content. CaO decreases during the final stage of processing because of increase in slag amount and increase in FeO content of the slag. Al_2O_3 gradually decreases throughout the blow period. The weight percent of SiO_2 slowly increases to 20 weight percent and then decreases because of an increase in FeO. Figure 2a, b shows the FactSage results of composition profile for hot metal and slag for BOF simulation heat 2, respectively. The explanations and reasons given for heat 1 profile are well applicable for heat 2.

Figures 3 and 4 show the validation of LRF simulation of LCRSS and MCRSS, respectively, with industrial data. Carbon, silicon, manganese and chromium at different stages of LRF for LCRSS and MCRSS are in good agreement with industry data and are presented in Figs. 3 and 4, respectively. However, phosphorous and sulfur have significant deviation from the FactSage-predicted values. Deviation of phosphorus is most likely arising due to the non-consideration of phosphorous in ferro-alloys and other sources like slag carryover [1, 14]. It is observed from the figure that sulfur deviates much from the simulation results only at the final stage, i.e., after sulfur wire injection. This may be attributed to the non-equilibrium state of free-cutting steels after sulfur wire injection. FactSage calculates every phase composition assuming that the slag–metal equilibrium is achieved. However, during industrial practice, enough time is not given to achieve slag–metal equilibrium in the bath. Therefore, it is inferred that slag–metal equilibrium is not allowed to be achieved and to simulate the same, slag system is removed from FactSage simulation, while Ca and S injection is carried out.

Slag composition for different stages of LRF process obtained using FactSage simulation is presented in Figs. 5 and 6 for LCRSS and MCRSS, respectively. It is observed from the figure that lime is constant for entire heat, as it is added in the initial stages of LRF process. Alumina gradually increases indicating aluminum deoxidation taking place before and during vacuum degassing. MgO in slag comes from refractory lining due to chemical and mechanical wear of the refractory. It is also observed from the graph that primary stages of refining, i.e., deoxidation and alloying, encourage more refractory erosion in comparison with later stages of the process. FeO and MnO in secondary slag are found to be very less in the final stage of LRF process in comparison with initial stages of the process.

Calcium–silicide wire injection and sulfur wire injection are important steps in producing ultraclean automobile Al killed steels such as fasteners grade (re-sulfur steel) [15–20]. Calcium treatment is mainly performed to modify solid alumina inclusions to increase it's floatability. Calcium also acts as the deep deoxidizer and deep desulfurizer apart from an inclusion modifier. This is attributed to the very high affinity of calcium toward sulfur and oxygen, and it forms CaS and CaO, respectively. In industry, sulfur is added after calcium treatment to avoid detrimental CaS formation, presuming that calcium could get consumed for modification of alumina inclusions. However, it creates an environment to generate complex oxysulfide inclusions at the end of LRF process. Hence, FactSage is used to

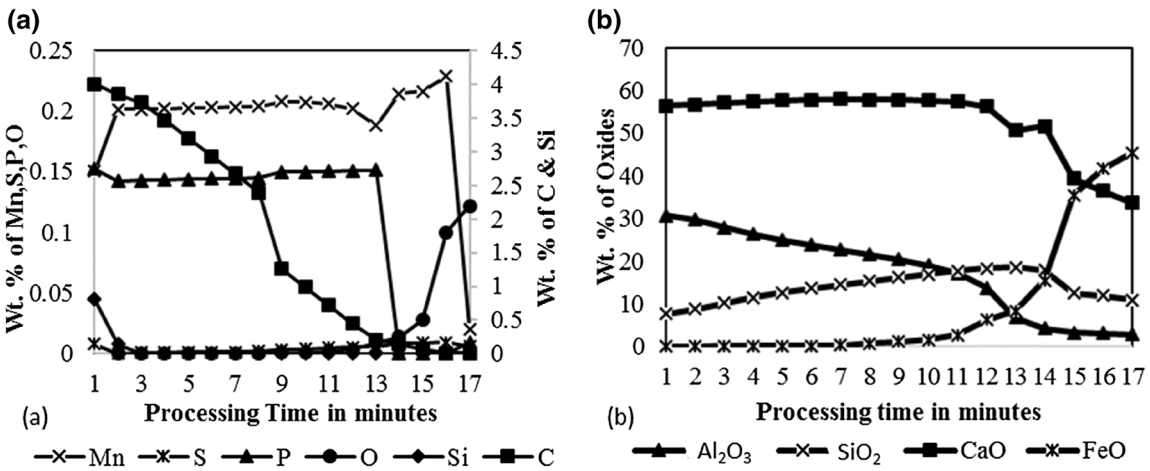

Fig. 2 FactSage-predicted hot metal **a** and slag **b** composition profile of BOF for heat 2

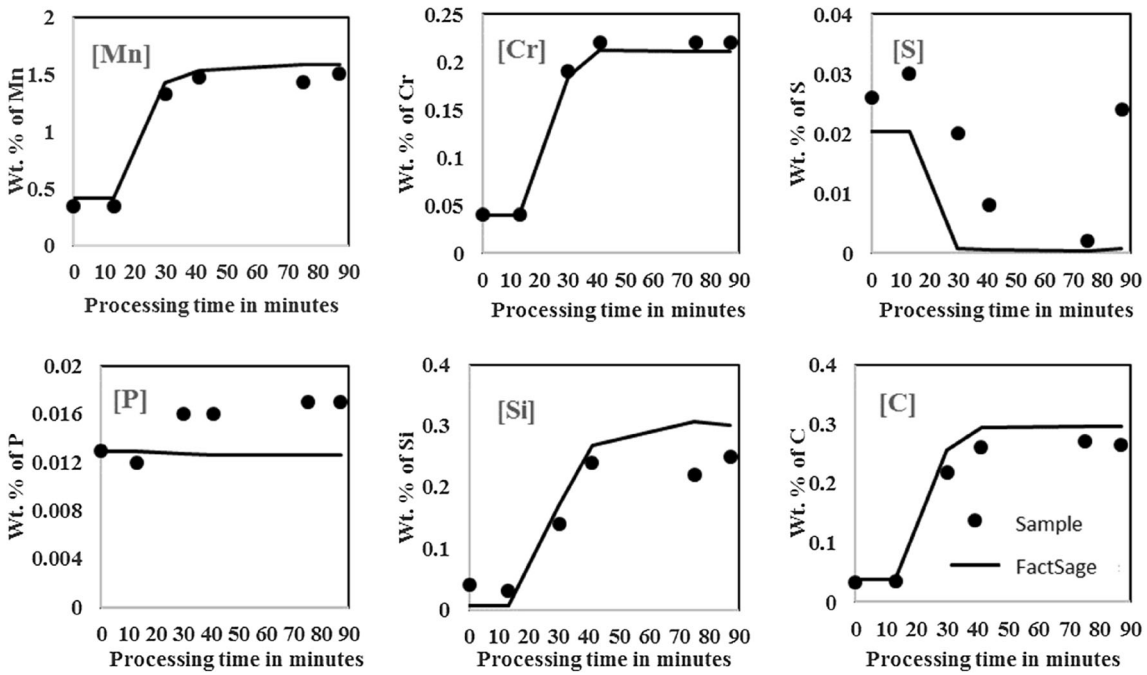

Fig. 3 Comparison of FactSage-predicted equilibrium composition with industrial samples' composition for LCRSS secondary refining (solid round points are industry value)

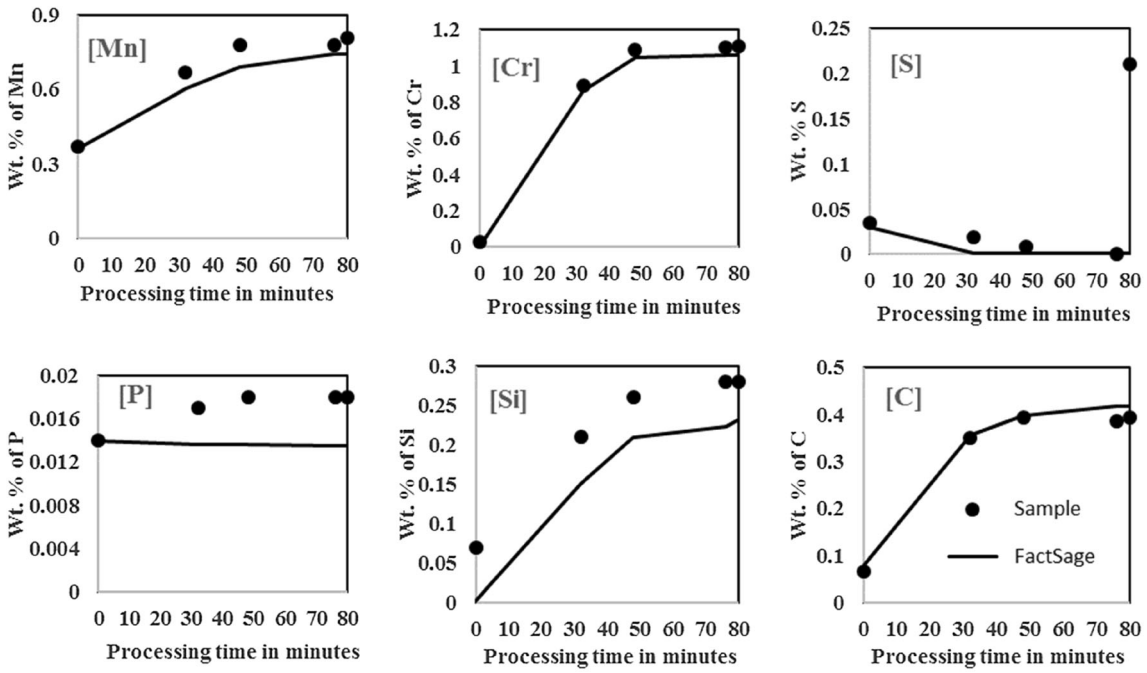

Fig. 4 Comparison of FactSage-predicted equilibrium composition with industrial samples' composition for MCRSS secondary refining (solid round points are industry value)

simulate the calcium and sulfur treatment to understand the phenomena in a better perspective with respect to their recoveries.

Figure 7a shows the variation of weight percent of calcium and sulfur content in liquid steel for varying calcium recovery during calcium treatment, as predicted by FactSage. It shows that an increase in calcium content in the liquid steel decreases the sulfur content in the steel. This is due to the chemical reaction and subsequent equilibrium between calcium and sulfur resulting in the formation of

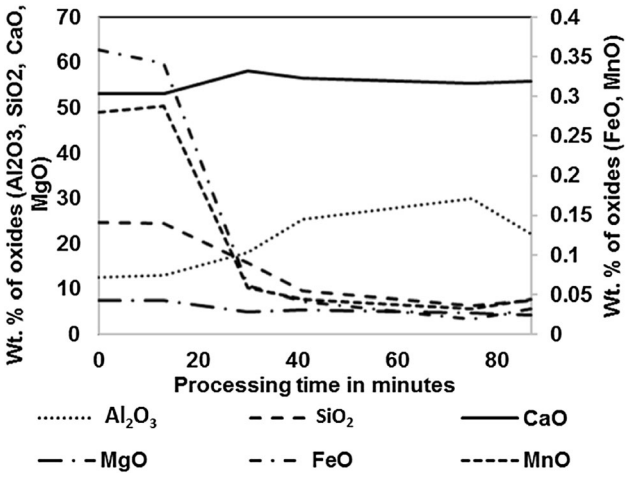

Fig. 5 FactSage-simulated equilibrium composition of slag for LCRSS secondary refining

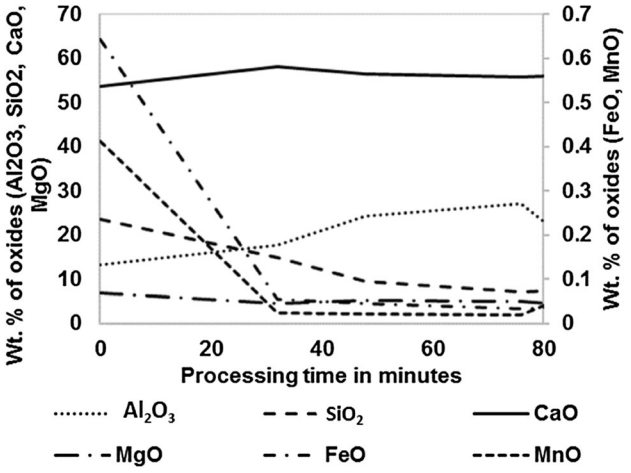

Fig. 6 FactSage-simulated equilibrium composition of slag for MCRSS secondary refining

CaS inclusion. Increasing calcium recovery increases dissolved calcium content in the liquid steel and decreases the dissolved sulfur content of the steel. There are not much differences noticed when comparing LCRSS and MCRSS, but MCRSS has lower calcium solubility at higher calcium recoveries than LCRSS. Maximum dissolved calcium content in the liquid steel obtained is 25 ppm, which occurs at 100% calcium recovery. It may be noted that higher dissolved calcium is not beneficial for re-sulfur steel, as it tends to form detrimental high melting CaS during further cooling and solidification of liquid steel. It may be beneficial for other normal steels which, demand very less sulfur level. Therefore, a compromising condition should be arrived between Ca and S present in the liquid steel to avoid detrimental CaS formation and at the same time, sufficient soluble calcium should be available to complete the conversion of detrimental alumina to calcium aluminates before solidification.

Figure 7b shows the amount of CaS and CaO formed during calcium treatment in liquid steel for varying calcium recovery. As already mentioned, Ca is a deep deoxidizer and deep desulfurizer, and it will form both CaO and CaS as it enters liquid steel. It can be seen from the graph that CaS formed in MCRSS grade is larger in amount than LCRSS grade. As it has been noted, the amount of dissolved sulfur and calcium increases the formation of CaS. The amount of CaO formed for both MCRSS and LCRSS does not change much. However, further addition of sulfur will react with CaO and form CaS and it may encourage clogging of SEN [9] during continuous casting of liquid steel. Figure 8 shows the variation of the weight of CaS solid precipitated in LCRSS and MCRSS during sulfur wire injection for various recovery of sulfur and calcium. As expected, the amount of CaS inclusion increases as

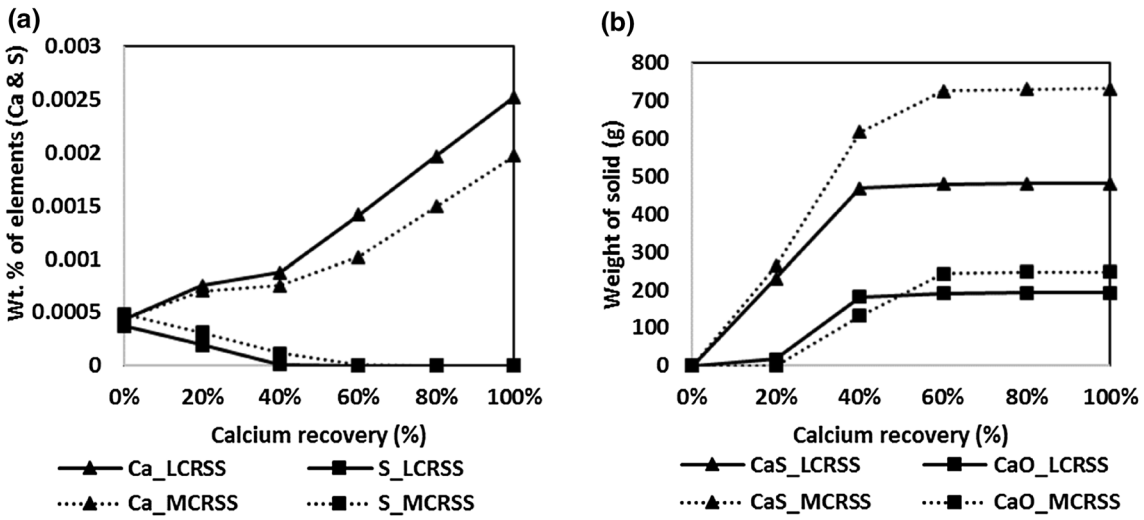

Fig. 7 Comparison of FactSage-calculated equilibrium composition of Ca and S (**a**) and comparison of FactSage-calculated equilibrium amount of solids formed (**b**) for various Ca recoveries

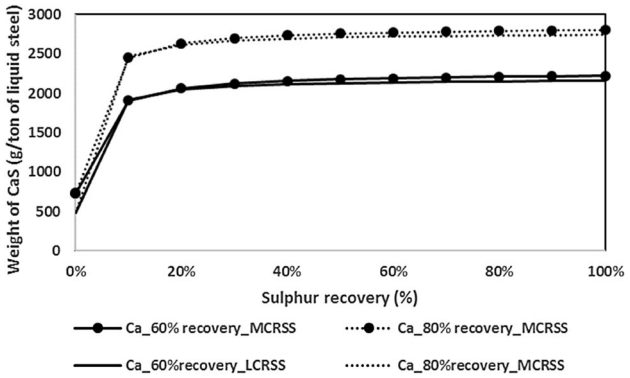

Fig. 8 FactSage-calculated equilibrium amount of solids (CaS) formed during sulfur wire injection for various Ca and S recoveries

sulfur and calcium recovery increases in the liquid bath. However, the formation of CaS or CaO is influenced by the presence of non-metallic inclusion and other dissolved elements in liquid steel. In the present investigation, the sulfur and calcium obtained in steel samples after wire injection are 24 and 6 ppm for LCRSS and 20 and 4 ppm for MCRSS, respectively. FactSage investigation reveals that 4–6 ppm of calcium in the steels corresponds to the sulfur recovery of less than 10% for the steelmaking practices, irrespective of LCRSS or MCRSS. However, 20–24 ppm sulfur corresponds to > 80% recovery during steelmaking practices. Complex behavior of sulfur and calcium during steelmaking practices and its understanding on interaction with inclusions in steel is very much necessary. The SEM micrograph of the steel samples collected after Ca and S treatment followed by 5 min of Ar rinsing is represented in Fig. 9. The figure shows the typical morphology of calcium treated alumina based non-metallic inclusion that is present in liquid steel. EDS analysis is shown in Fig. 9b, d that corresponds to the non-metallic inclusion given in Fig. 9a, c, respectively. From the intensity of EDS peak presented in Fig. 9, it could be concluded that extent of the chemical as well as morphology modification by Ca treatment is better for LCRSS than MCRSS. The Al/Ca ratio for LCRSS and MCRSS is found to be 1.25 and 2.28, respectively. It is observed from the present investigation that even 2 ppm of difference in calcium in liquid steel have the significant effect in modification (chemical as well as morphology) of non-metallic inclusions, which is further expected to influence the downstream processing and mechanical properties of

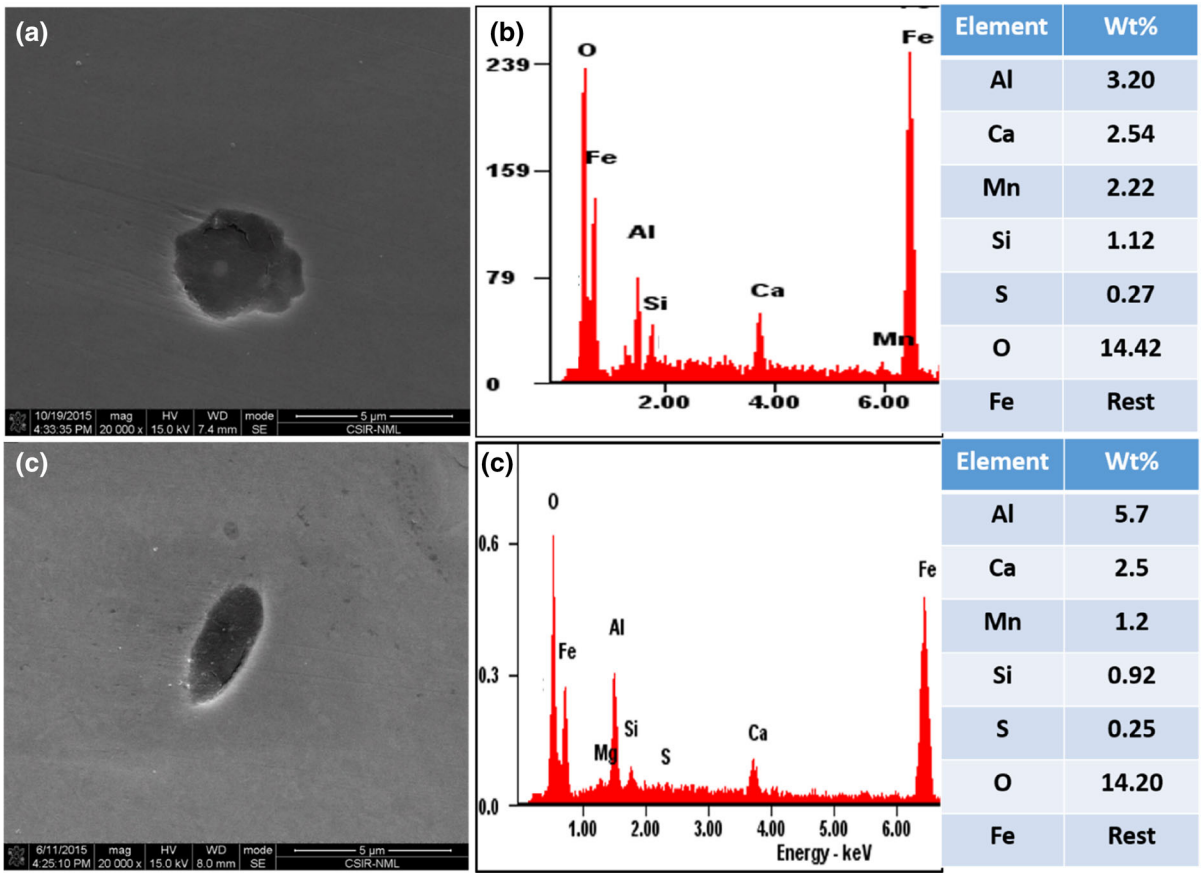

Element	Wt%
Al	3.20
Ca	2.54
Mn	2.22
Si	1.12
S	0.27
O	14.42
Fe	Rest

Element	Wt%
Al	5.7
Ca	2.5
Mn	1.2
Si	0.92
S	0.25
O	14.20
Fe	Rest

Fig. 9 SEM micrograph of non-metallic inclusion present in **a** LCRSS and **c** MCRSS and their EDS determined compositions in **b** and **d**, respectively

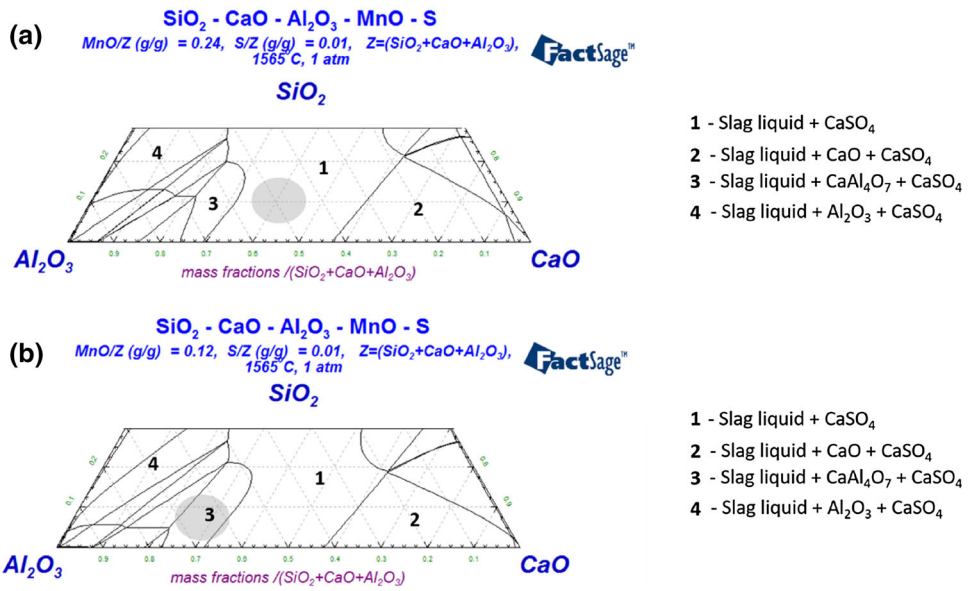

Fig. 10 Domain area (gray color) of non-metallic inclusion present in LCRSS **a** and MCRSS **b** using FactSage-generated ternary plot

steels. After normalizing the composition of non-metallic inclusion in steels, the composition of inclusions is plotted in FactSage-generated $CaO–SiO_2–Al_2O_3$ pseudo-ternary phase diagram with constant MnO and S for LCRSS and MCRSS separately, and is presented in Fig. 10. The gray round area represented in the ternary diagram shows the average composition of analyzed non-metallic inclusions in both the steel grades. It clearly shows that average composition of non-metallic inclusion after calcium and sulfur treatment falls on liquid plus $CaSO_4$ region for LCRSS. However, it falls on liquid + $CaSO_4$ + $CaAl_4O_7$ region for MCRSS. It is instructive to note that liquid slag with oxides generally increases the viscosity and tends to behave as a solid phase in a liquid medium. The average size of the inclusion in LCRSS is comparatively bigger than MCRSS due to high viscosity and solid behavior of non-metallic inclusion in liquid steel. Therefore, the tendency of floatation of such complex oxysulfide inclusions will be difficult in MCRSS and cause the SEN clogging as well as impaired cleanliness of steel.

5 Conclusions

In the present investigation, FactSage was utilized to simulate the high-temperature metallurgical processes such as BOF refining and ladle refining process and some insights have been given on calcium and sulfur injection during the last stage of ladle refining operation. It could be concluded that process charts pertaining to liquid steel and slag composition variation during refining in BOF similar to the standard ones were obtained and discussed. Simulation of ladle refining practice was done, and the results were validated with the industry data. Evolution of slag composition during ladle refining process of free-cutting steel was also established using FactSage. A special insight has been given to understand the solubility of Ca and S along with the formation of solid products such as CaO and CaS during inclusion modification and discussed. This investigation gave an improved understanding about the re-sulfurization of liquid steel by conducting systematic experimental as well as simulation study using FactSage to address industrial issues like clogging.

References

1. Ghosh A, and Chatterjee A, *Iron Making and Steelmaking: Theory and Practices*. PHI Publication (2008).
2. Jung I-H *Iron Mak Steelmak: Theory Pract* **34** (2010) 332
3. Van Ende M-A, and Jung I-H, *Miner Met Mater Soc ASM Int* (2016). https://doi.org/10.1007/s11663-016-0698-6
4. Kamaraj A, Mandal G K, and Bandyopadhyay D, *Trans Ind Inst Met* **68** (2015) 9
5. Kamaraj A, Mandal G K, Minj R K, Misra S, and Bandyopadhyay D, *Trans Ind Inst Met* **70** (2017) 1887
6. Li Z, Wang X-H, and Jia W, *J Iron Steel Res Int* **21** (2014) 70.
7. Cui H-Z, and Chen W-Q, *J Iron Steel Res Int* **19** (2012) 22.
8. Holappa L E K, and Helle A S, *J Mater Process Technol* **53** (1995) 177.
9. Cheng Z-J, Guo J, and Cheng S-S, *J Iron Steel Res. Int* **20** (2013) 14
10. Yang S-F, Li J-S, Wang Z-F, Li J, and Lin L, *Int J Miner Metall Mater* **18** (2011) 18
11. He S, Chen G, Guo Y, Shen B, and Wang Q, *Metall Mater Trans B* **46** (2015) 585
12. Yang S-F, Li J-S, Zhang L-F, Kent P, and Wang Z-F, *J Iron Steel Res Int* **17** (2010) 01.
13. Shi C-B, Yu W-T, Wang H, Li J, and Jiang M, *Metall Mater Trans B*, **46** (2016) 146.

14. Fruehan R J, *Ladle Metallurgy Principles and Practices: Iron and Steel Society of AIME Publication* (1974).
15. Faulring G M, and Ramalingam S, *Metall Mater Trans B*, **11** (1979) 125.
16. Kamaraj A, Venkatesan J, and Venkatakrishnan P G, *Adv Mater Res* **585** (2012) 364.
17. Brandaleze E, Hereñú S, Tormo J, and Alvarez Armas I, *Ironmak Steelmak* **40** (2013) 216.
18. Knutsen, R D, and Hutchings R, *Mater Sci Technol*, **4** (1988) 127.
19. Li Y-D, Li C-J, Li C-L, and Jiang M-F, *J Iron Steel Res Int* **22** (2015) 457.
20. Xu J, Huang F, and Wang X, *Metall Mater Trans B* **47** (2016) 1217.